

# Energy and angular distributions of the bottom quark in the electron-positron annihilation $e^+e^- \rightarrow bW^+\bar{t}$

Ivan V. Truten<sup>1,\*</sup> and Alexander Yu. Korchin<sup>1,2,†</sup>

<sup>1</sup>*NSC ‘Kharkiv Institute of Physics and Technology’, 61108 Kharkiv, Ukraine*

<sup>2</sup>*V.N. Karazin Kharkiv National University, 61022 Kharkiv, Ukraine*

(Dated: December 22, 2024)

The distributions of the bottom quark in the process  $e^+e^- \rightarrow t\bar{t} \rightarrow bW^+\bar{t}$  are considered at the  $e^+e^-$  energy corresponding to the first construction stage of the Compact Linear Collider. The cross sections of  $e^+e^- \rightarrow b\dots$ , as functions of the  $b$ -quark energy and angle with respect to the direction of the electron beam, are derived and calculated. The effects of physics beyond the Standard Model are included via the modified  $\gamma t\bar{t}$  and  $Zt\bar{t}$  couplings which naturally appear in effective field theories. In addition to the cross sections, the energy and angular asymmetries are calculated. The dependence of these observables on the  $e^+e^-$  energy is calculated, and features of this dependence is investigated.

PACS numbers: 11.30.Er, 12.15.Ji, 12.60.Fr, 14.80.Bn

## I. INTRODUCTION

Nowadays the global interest in particle physics is the search for “new physics”, or physics beyond the Standard Model (SM). An important direction of research is study of properties of the top quark. These properties are planned to be explored precisely on future electron-positron colliders, such as International Linear Collider (ILC) [1] and Compact Linear Collider (CLIC) [2–4]. The ILC will start at the center-of-mass energy of 250 GeV followed by 500 GeV upgrade [4, 5]. The CLIC promises to be a good candidate for production of the on-mass-shell top quark and studying its properties. At the first construction stage of the CLIC, the center-of-mass energy will be 380 GeV with expected integrated luminosity of  $1 \text{ ab}^{-1}$ , which will include  $100 \text{ fb}^{-1}$  collected near the  $t\bar{t}$  production threshold [3, 4, 6].

The present work is a continuation of our previous paper [7], where the polarization of the top quark, produced in electron-positron annihilation, was studied in detail with emphasis on physics beyond the SM (BSM). The aim of the present paper is to consider the consequent decay of the top quark  $e^+e^- \rightarrow t\bar{t} \rightarrow bW^+\bar{t}$ . Clearly, the observables related to the bottom quark are more appropriate for the future experimental investigations.

Note that this reaction was studied in the papers [8–11], where the distributions of the lepton, coming from the decay  $W^+ \rightarrow \ell^+\nu_\ell$ , was evaluated. The issue of a possible  $CP$  violation was studied.  $CP$  violation in framework of the MSSM was discussed and estimated in the spectra of the bottom quark in Refs. [12–15].

In the present paper, we concentrate on distributions of the bottom quark. In addition to the SM, we take into account the BSM effects which are described by the anomalous interactions of the photon and  $Z$  boson with the top quark. These interactions naturally appear in effective field theory (EFT) Lagrangian (see, e.g., [16]), which contains both the SM Lagrangian and the higher-dimensional terms beyond the SM. The calculations in our paper are performed using the formalism developed in Ref. [17] which allows one to find in a compact form distributions of the secondary particles, such as the bottom quark in  $e^+e^- \rightarrow t\bar{t} \rightarrow bW^+\bar{t}$ .

---

\*Electronic address: [i.truten@kipt.kharkov.ua](mailto:i.truten@kipt.kharkov.ua)

†Electronic address: [korchin@kipt.kharkov.ua](mailto:korchin@kipt.kharkov.ua)

We investigate effects of the BSM couplings  $\kappa$  and  $\kappa_z$ , which determine the anomalous  $\gamma t\bar{t}$  and  $Z t\bar{t}$  vertices, and influence of the polarization of the top quark arising in the  $e^+e^- \rightarrow t\bar{t}$  process on the energy and angular distributions of the  $b$  quark. In this connection note, that in framework of the SM, the distribution of the bottom quark was analytically derived in [9] for the unpolarized leptons and in [18] for the longitudinally polarized leptons. In the present work we perform calculation beyond the SM, where analytical consideration is rather cumbersome, and using the formalism [17] facilitates calculations.

The structure of the paper is as follows. In Section II theoretical basis for calculation of the process  $e^+e^- \rightarrow b\dots$  is overviewed. Two possible ways of calculation of the cross section suggested in [17] are mentioned. We also introduce polarization vector of the top quark which arises in the production process  $e^+e^- \rightarrow t\bar{t}$  [7]. In Subsection II A the cross section of  $e^+e^- \rightarrow b\dots$  is considered as a function of the bottom-quark energy  $E_b$ , while in Subsection II B the cross section is obtained as a function of the polar angle  $\theta_b$  between the momentum of  $b$  quark and direction of electron beam. In Section III results of calculation in the SM and BSM of the  $e^+e^- \rightarrow b\dots$  cross sections as functions of the energy  $E_b$  and the angle  $\theta_b$  are presented. The BSM results are obtained for some values of the coupling constants  $\kappa$  and  $\kappa_z$ . Several observables, such as normalized energy and angle distributions, and energy and angular asymmetries are studied at various values of  $\kappa$  and  $\kappa_z$ . Dependence of asymmetries on the  $e^+e^-$  invariant energy is investigated. In Section IV conclusions are given.

## II. FORMALISM FOR THE PROCESS $e^+e^- \rightarrow bW^+\bar{t}$

Let us consider electron-positron annihilation into a pair of top quarks, where one of the quarks decays,  $t \rightarrow bW^+$ , *i.e.* the process  $e^+e^- \rightarrow t\bar{t} \rightarrow bW^+\bar{t}$ . To calculate the energy and the angular distribution of the  $b$  quark one can use efficient formalism of Refs. [8, 17]. According to these articles there are two equivalent ways of calculation of the cross section of interest. In the first way the cross section is written as

$$d\sigma(e^+e^- \rightarrow bW^+\bar{t}) = \int \frac{d\sigma(e^+e^- \rightarrow t\bar{t}; 0)}{d\Omega_t} \frac{d\Gamma(t \rightarrow bW^+; a^\mu)}{\Gamma} d\Omega_t, \quad (1)$$

where  $d\sigma(e^+e^- \rightarrow t\bar{t}; 0)/d\Omega_t$  is the differential cross section of the electron-positron annihilation to the top quarks, which is calculated for all unpolarized particles.  $d\Gamma(t \rightarrow bW^+; a^\mu)$  is the differential width of the decay of the polarized top quark, where its polarization arises in the process  $e^+e^- \rightarrow t\bar{t}$  and is described by the four-vector  $a^\mu$ . The cross section is calculated in the center-of-mass (CM) frame, while the  $t \rightarrow bW^+$  differential decay width and the total width  $\Gamma$  are evaluated in the top-quark rest frame.

The second way of calculation implies that the cross section can be presented as

$$d\sigma(e^+e^- \rightarrow bW^+\bar{t}) = \int \frac{d\sigma(e^+e^- \rightarrow t\bar{t}; n^\mu)}{d\Omega_t} \frac{d\Gamma(t \rightarrow bW^+; 0)}{\Gamma} d\Omega_t, \quad (2)$$

where the  $e^+e^- \rightarrow t\bar{t}$  differential cross section is calculated for the polarized top quark with the polarization four-vector  $n^\mu$ :

$$n^\mu = \alpha_b \left( \frac{p_b^\mu m_t}{p_t \cdot p_b} - \frac{p_t^\mu}{m_t} \right), \quad p_t \cdot n = 0, \quad n \cdot n = -\alpha_b^2, \quad (3)$$

where  $p_t^\mu$  ( $p_b^\mu$ ) is the four-momentum of the top (bottom) quark. The  $t \rightarrow bW^+$  decay width in (2) is calculated for the unpolarized top quark. The parameter  $\alpha_b$  determines the asymmetry in the decay  $t \rightarrow bW^+$  of the polarized top quark.

Further we will mainly use the form in Eq. (1), since only the  $e^+e^- \rightarrow t\bar{t}$  unpolarized cross section enters, while the polarization vector  $a^\mu$  of the produced top quark was already calculated in [7]. In Sec. III we check explicitly the equivalence of the cross sections in Eqs. (1) and (2).

Let us discuss the distribution of the bottom quark. In general, the differential decay width of  $t \rightarrow b W^+$  is

$$d\Gamma = \frac{1}{2m_t} |\mathcal{M}|^2 dX_{LIPS} \quad (4)$$

with  $dX_{LIPS}$  being the Lorentz invariant phase space, and the matrix element squared for the polarized top quark, and the unpolarized  $W$  boson and  $b$  quark reads

$$|\mathcal{M}|^2 = \sqrt{2} G_F N |V_{tb}|^2 (1 + \alpha_b \vec{P} \vec{n}_{b,R}) = \sqrt{2} G_F N |V_{tb}|^2 \left( 1 - \alpha_b \frac{m_t a \cdot p_b}{p_t \cdot p_b} \right), \quad (5)$$

where  $G_F$  is the Fermi weak constant,  $V_{tb} \approx 1$  is the element of the CKM matrix, and

$$N = (m_t^2 - m_W^2)(2m_W^2 + m_t^2), \quad \alpha_b = \frac{2m_W^2 - m_t^2}{2m_W^2 + m_t^2} = -0.40. \quad (6)$$

Here  $m_t$  ( $m_W$ ) is the mass of the top quark ( $W$  boson) and we neglect the bottom-quark mass, *i.e.* put  $m_b = 0$ . Note that Eq. (5) is written both in the rest frame of the top quark (denoted by the subscript ‘R’) and in the Lorentz-invariant form. In the frame ‘R’,  $\vec{n}_{b,R}$  is the unit vector in the direction of the  $b$ -quark momentum, and the  $t$ -quark polarization is determined by the three-vector  $\vec{P}$ , such that  $a_R^\mu = (0, \vec{P})$ . In the frame, where  $t$  quark moves with the momentum  $\vec{p}_t$  and energy  $E_t$ , the polarization four-vector reads [19]

$$a^\mu = \left( \frac{\vec{P} \vec{p}_t}{m_t}, \vec{P} + \frac{\vec{p}_t (\vec{P} \vec{p}_t)}{m_t (m_t + E_t)} \right), \quad a \cdot p_t = 0, \quad a \cdot a = -\vec{P}^2. \quad (7)$$

The total decay width is

$$\Gamma = \frac{p_b^0 G_F |V_{tb}|^2 N}{4\sqrt{2}\pi m_t^2}, \quad (8)$$

where  $p_b^0 = (m_t^2 - m_W^2)/2m_t$  is the bottom-quark momentum (energy) in the  $t$ -quark rest frame.

The two-particle phase space,

$$dX_{LIPS} = (2\pi)^4 \delta^4(p_t - p_b - p_W) \frac{d^3 p_b}{(2\pi)^3 2E_b} \frac{d^3 p_W}{(2\pi)^3 2E_W}, \quad (9)$$

where  $E_b$  and  $E_W$  is the energy of the bottom quark and  $W$  boson, respectively, allows one to integrate over the  $W$ -boson momentum and obtain

$$\frac{1}{\Gamma} d\Gamma(t \rightarrow b W^+, a^\mu) = \frac{m_t}{4\pi p_b^0} \left( 1 - \alpha_b \frac{m_t a \cdot p_b}{p_t \cdot p_b} \right) \delta(E_t - E_b - E_W) \frac{E_b}{E_W} dE_b d\Omega_b \quad (10)$$

with  $E_W = (m_W^2 + \vec{p}_t^2 + E_b^2 - 2\vec{p}_t \vec{p}_b)^{1/2}$  and  $E_b = |\vec{p}_b|$ . Substitution of (10) in (1) gives the required cross section

$$d\sigma(e^+ e^- \rightarrow b W^+ \bar{t}) = \frac{m_t}{4\pi p_b^0} \int \frac{d\sigma(e^+ e^- \rightarrow t \bar{t}; 0)}{d\Omega_t} \left( 1 - \alpha_b \frac{m_t a \cdot p_b}{p_t \cdot p_b} \right) \delta(E_t - E_b - E_W) \frac{E_b}{E_W} dE_b d\Omega_b d\Omega_t, \quad (11)$$

from which one can obtain the energy and angular distributions of the bottom quark for arbitrary  $e^+ e^- \rightarrow t \bar{t}$  cross section.

### A. Energy spectrum of the bottom quark

For this case the coordinate system is chosen as shown in Fig. 1 (left): the top-quark (and antiquark) momentum is directed along the  $OZ'$  axis, the electron (and positron) momentum lies in the  $X'OZ'$  plane, the bottom-quark momentum points in arbitrary direction. Further,  $\theta_t$  is the angle between the electron and the top-quark momenta,  $\theta'_b$  is the angle between  $\vec{p}_t$  and  $\vec{p}_b$ .

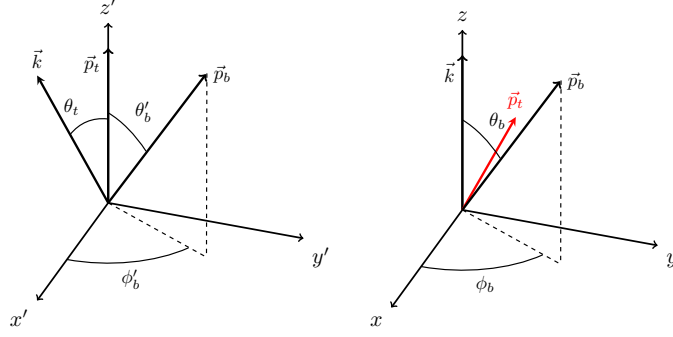


Figure 1: The coordinate systems used for the energy distribution (left side) and the angular distribution (right side) of the bottom quark.

In the CM frame, the four-momenta of  $e^-$ ,  $t$  and  $b$  quarks, and polarization vector are

$$\begin{aligned}
 k^\mu &= E_t(1, \sin \theta_t, 0, \cos \theta_t), \\
 p_t^\mu &= E_t(1, 0, 0, V), \\
 p_b^\mu &= E_b(1, \sin \theta'_b \cos \phi'_b, \sin \theta'_b \sin \phi'_b, \cos \theta'_b), \\
 a^\mu &= (\gamma V P_{z'}, P_{x'}, P_{y'}, \gamma P_{z'}),
 \end{aligned} \tag{12}$$

where  $V = p_t/E_t$  is the velocity of the top quark, and  $\gamma = E_t/m_t$  is the Lorentz factor. The components of the polarization vector  $\vec{P} = (P_{x'}, P_{y'}, P_{z'})$  have been evaluated in Ref. [7] as functions of the top-quark angle  $\theta_t$ . Then one can carry out integration in Eq. (11) over the angles of the  $b$  quark  $\theta'_b$  and  $\phi'_b$ , and the cross section as a function of the bottom-quark energy becomes

$$\frac{d\sigma(e^+e^- \rightarrow b\dots)}{dE_b} = \frac{1}{2\gamma V p_b^0} \int_{-1}^{+1} \frac{d\sigma(e^+e^- \rightarrow t\bar{t}; 0)}{d\cos\theta_t} \left[ 1 + \frac{\alpha_b P_{z'}(\theta_t)}{V} \left( \frac{E_b}{\gamma p_b^0} - 1 \right) \right] d\cos\theta_t, \tag{13}$$

where the energy varies within the limits

$$E_- \leq E_b \leq E_+, \quad E_\pm = \frac{p_b^0}{\gamma(1 \mp V)}. \tag{14}$$

It is seen that only the longitudinal component of the quark polarization survives after integration over the azimuthal angle  $\phi'_b$ . The cross section in Eq. (13) is linear in the energy  $E_b$ , if we keep the polarization of the top quark. If polarization is neglected, *i.e.*  $\vec{P} = 0$ , the cross section (13) is independent of the  $b$ -quark energy. In the SM, this feature was pointed out in Ref. [18], and apparently this is a general property of the energy spectrum regardless of a model for  $e^+e^- \rightarrow t\bar{t}$ . It is also interesting that the  $t$ -quark polarization does not contribute at the  $b$ -quark energy  $\tilde{E}_b = \gamma p_b^0$ , as is seen from the last term in (13).

As a check of Eq. (13) we can calculate the total cross section by integrating (13) over  $E_b$ . Then use of (14) yields

$$\int_{E_-}^{E_+} \frac{d\sigma(e^+e^- \rightarrow b\dots)}{dE_b} dE_b = \int_{-1}^{+1} \frac{d\sigma(e^+e^- \rightarrow t\bar{t}; 0)}{d\cos\theta_t} d\cos\theta_t = \sigma(e^+e^- \rightarrow t\bar{t}), \tag{15}$$

which is the normalization of the cross section.

## B. Angular spectrum of the bottom quark

It is convenient to define the angular distribution of the bottom quark in the coordinate system shown in Fig. 1 (right). In this system the polar angle of the  $b$  quark is determined with respect to the direction of the electron beam which is parallel to the  $OZ$  axis. The  $b$ -quark momentum is defined by the polar angle  $\theta_b$  and the azimuthal angle  $\phi_b$ .

The system in Fig. 1 (right) is obtained from the system in Fig. 1 (left) by the clockwise rotation around the  $OY'$  axis on the angle  $\theta_t$ , so that

$$\begin{pmatrix} x \\ y \\ z \end{pmatrix} = \begin{pmatrix} \cos \theta_t & 0 & -\sin \theta_t \\ 0 & 1 & 0 \\ \sin \theta_t & 0 & \cos \theta_t \end{pmatrix} \begin{pmatrix} x' \\ y' \\ z' \end{pmatrix}, \quad (16)$$

where  $x', y', z'$  are the primary non-rotated axes and  $x, y, z$  are the rotated ones. The four-momenta of the particles and the polarization vector take the form

$$\begin{aligned} k^\mu &= E_t(1, 0, 0, 1), \\ p_t^\mu &= E_t(1, -V \sin \theta_t, 0, V \cos \theta_t), \\ p_b^\mu &= E_b(1, \sin \theta_b \cos \phi_b, \sin \theta_b \sin \phi_b, \cos \theta_b), \\ a^\mu &= (\gamma V P_{z'}, P_{x'} \cos \theta_t - \gamma P_{z'} \sin \theta_t, P_{y'}, P_{x'} \sin \theta_t + \gamma P_{z'} \cos \theta_t), \end{aligned} \quad (17)$$

and for the scalar product  $a \cdot p_b$  in (11) we find

$$a \cdot p_b = E_b [P_{z'} \gamma (V - \cos \Theta_{\vec{p}_t \vec{p}_b}) - P_{x'} (\cos \theta_t \sin \theta_b \cos \phi_b + \sin \theta_t \cos \theta_b) - P_{y'} \sin \theta_b \sin \phi_b], \quad (18)$$

$$\cos \Theta_{\vec{p}_t \vec{p}_b} \equiv \cos \theta_t \cos \theta_b - \sin \theta_t \sin \theta_b \cos \phi_b. \quad (19)$$

Performing integration in (11) over the energy  $E_b$  and the azimuthal angle  $\phi_b$ , we obtain the cross section as a function of the polar angle of the bottom quark

$$\begin{aligned} \frac{d\sigma(e^+e^- \rightarrow b \dots)}{d \cos \theta_b} &= \frac{1}{4\pi\gamma^2} \int_{-1}^{+1} d \cos \theta_t \frac{d\sigma(e^+e^- \rightarrow t \bar{t}; 0)}{d \cos \theta_t} \int_0^{2\pi} d\phi_b \frac{1}{(1 - V \cos \Theta_{\vec{p}_t \vec{p}_b})^2} \\ &\times \left[ 1 - \alpha_b \frac{P_{z'}(\theta_t) \gamma (V - \cos \Theta_{\vec{p}_t \vec{p}_b}) - P_{x'}(\theta_t) (\cos \theta_t \sin \theta_b \cos \phi_b + \sin \theta_t \cos \theta_b) - P_{y'}(\theta_t) \sin \theta_b \sin \phi_b}{\gamma (1 - V \cos \Theta_{\vec{p}_t \vec{p}_b})} \right]. \end{aligned} \quad (20)$$

The normalization of this cross section is

$$\int_{-1}^{+1} \frac{d\sigma(e^+e^- \rightarrow b \dots)}{d \cos \theta_b} d \cos \theta_b = \sigma(e^+e^- \rightarrow t \bar{t}; 0). \quad (21)$$

### III. RESULTS OF CALCULATION AND DISCUSSION

#### A. Cross sections

The considered process on the tree level is described by the Feynman diagrams in Fig. 2. We start with description of this process in the framework of the SM without radiative corrections (RC) to the vertices  $\gamma t \bar{t}$  and  $Z t \bar{t}$ , that corresponds to  $\kappa = \kappa_z = 0$ . Then we add RC in the SM by choosing nonzero values of  $\kappa$  and  $\kappa_z$ , and finally include anomalous couplings of quarks with the photon and  $Z$  boson related to the BSM physics. Thus the structure of the  $\gamma t \bar{t}$  and  $Z t \bar{t}$  vertices is chosen in the form

$$\begin{aligned} \Gamma_{\gamma t \bar{t}}^\mu &= -ie \left[ Q_t \gamma^\mu + i \frac{\sigma^{\mu\nu} q_\nu}{2m_t} (\kappa + i \tilde{\kappa} \gamma_5) \right], \\ \Gamma_{Z t \bar{t}}^\mu &= -i \frac{g}{2 \cos \theta_w} \left[ \gamma^\mu (v_t - a_t \gamma_5) + i \frac{\sigma^{\mu\nu} q_\nu}{2m_t} (\kappa_z + i \tilde{\kappa}_z \gamma_5) \right], \end{aligned} \quad (22)$$

where  $e$  is the positron charge,  $g = e/\sin \theta_w$  with  $\theta_w$  denoting the weak mixing angle,  $Q_t = 1/3$ ,  $v_t = 1/2 - 4/3 \sin^2 \theta_w$ ,  $a_t = 1/2$ , and  $q^\nu = k^\nu + k'^\nu$  is the four-momentum of the intermediate photon ( $Z$  boson). In the following we neglect the terms proportional to  $\tilde{\kappa}$  and  $\tilde{\kappa}_z$  in (22) responsible for the  $CP$ -violation and keep only the couplings  $\kappa$  and  $\kappa_z$

related respectively to the magnetic and weak magnetic dipole moments of the  $t$  quark. For details on relation of these couplings to the Wilson coefficients in the EFT Lagrangian and some constraints on their values see Ref. [7].

RC in the SM to the  $\gamma t\bar{t}$  and  $Zt\bar{t}$  vertices are contained in Eqs. (22) if one chooses the corresponding values,  $\kappa_{RC}$  and  $\kappa_{z,RC}$ . In this work we do not take into account other RC to the  $e^+e^- \rightarrow t\bar{t}$  reaction, as well as to the  $t \rightarrow bW^+$  decay. For  $e^+e^- \rightarrow t\bar{t}$ , certain RC have been studied in Refs. [20–24].

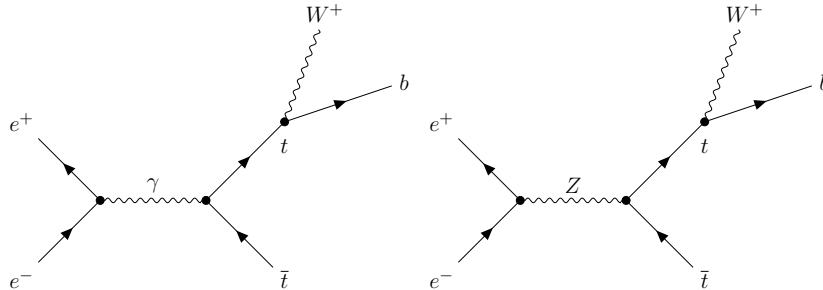


Figure 2: Feynman diagrams for  $e^+e^- \rightarrow bW^+t$  reaction. The vertices  $\gamma t\bar{t}$  and  $Zt\bar{t}$  can include RC and BSM couplings.

The calculated cross section (13) is shown in Fig. 3. The energy of the bottom quark lies in the interval  $43.7 \text{ GeV} \leq E_b \leq 105.3 \text{ GeV}$ . We present two variants of the calculation: the first one corresponds to neglect of the  $t$ -quark polarization,  $\vec{P} = 0$  (called “depolarized” process), and the second one corresponds to inclusion of the polarization,  $\vec{P} \neq 0$  (called “polarized” process).

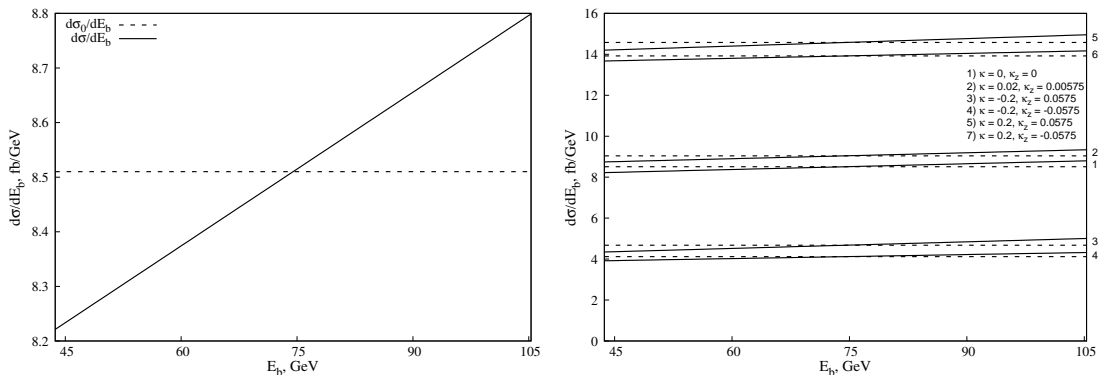


Figure 3: The cross section of the process  $e^+e^- \rightarrow b\dots$  as a function of the bottom-quark energy at the  $e^+e^-$  energy  $\sqrt{s} = 380 \text{ GeV}$ . Solid (dashed) curves correspond to the polarized (depolarized) process. Left side shows calculation in the SM with  $\kappa = \kappa_z = 0$ . Right side corresponds to various values of the couplings  $\kappa$  and  $\kappa_z$ .

The solid and dashed curves cross at the energy  $\tilde{E}_b = \gamma p_b^0 = (E_+ + E_-)/2 = 74.5 \text{ GeV}$ . The slope of the solid line in the SM appears to be  $9.4 \times 10^{-3} \text{ fb/GeV}^2$ . In Fig. 3 (right) we show calculation with several values of the couplings  $\kappa$  and  $\kappa_z$ . Firstly, note that the cross section varies considerably when changing the BSM couplings, and secondly, the difference between the polarized and depolarized cases is similar to the SM calculation in Fig. 3 (left), but the slope of the solid curves depends on the couplings. This is demonstrated in Table I.

The values of the couplings in Table I and in Fig. 3 are chosen as in Ref. [7]. Namely, in the first line, the values correspond to the SM without RC ( $\kappa = \kappa_z = 0$ ), while the second line includes RC in the SM in Eqs. (22) ( $\kappa_{RC} = 0.02$ ,  $\kappa_{z,RC} = 0.00575$ ). The latter were evaluated in Ref. [25] to the two loops in QCD and to the lowest order in electroweak couplings. The other values in Table I are chosen ten times bigger than  $\kappa_{RC}$  and  $\kappa_{z,RC}$ , as some conservative estimate. Since the sign of the BSM couplings is not known, the negative signs are also included in

Table I and Fig. 3. It is seen that the slope of the energy distribution depends on the BSM couplings, although the dependence is weak, at least for the considered moderate values of  $\kappa$  and  $\kappa_z$ .

Table I: The slope of the cross section  $d\sigma(e^+e^- \rightarrow b\dots)/dE_b$  for various couplings  $\kappa$ ,  $\kappa_z$ . The  $e^+e^-$  invariant energy is 380 GeV.

$\kappa$	$\kappa_z$	slope, $10^{-3}$ fb/GeV <sup>2</sup>
0.0	0.0	9.4
0.02	0.00575	9.7
0.2	0.0575	12.2
0.2	-0.0575	8.0
-0.2	0.0575	10.7
-0.2	-0.0575	6.6

In Fig. 4 we show the angular spectrum of the  $b$  quark (20). One can notice that in all calculations the solid and dashed curves cross at the point close to the angle  $\tilde{\theta} \approx \pi/2$ . As can also be seen from Fig. 4, the difference between the polarized and depolarized processes is more pronounced than the corresponding effect in the energy dependence in Fig. 3. Apparently the angular dependence is more sensitive to the top-quark polarization.

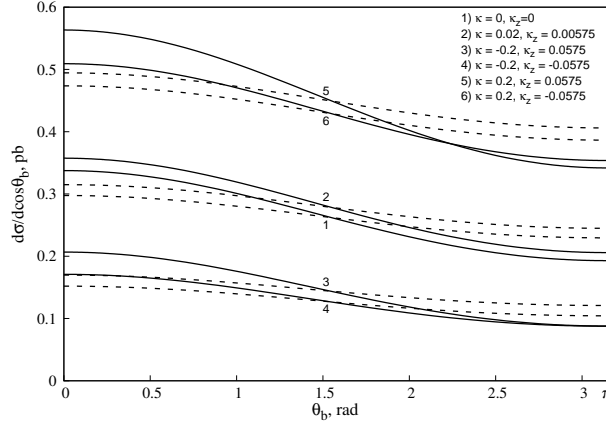


Figure 4: The cross section of the process  $e^+e^- \rightarrow b\dots$  as a function of the  $b$ -quark polar angle: (1) in the SM without RC, (2) in the SM with RC, and (3)-(6) beyond the SM. Solid (dashed) curves correspond to the polarized (depolarized) process.

It is of interest to plot the energy and angular normalized distributions

$$W(E_b) \equiv \frac{1}{\sigma(e^+e^- \rightarrow t\bar{t})} \frac{d\sigma(e^+e^- \rightarrow b\dots)}{dE_b}, \quad (23)$$

$$W(\theta_b) \equiv \frac{1}{\sigma(e^+e^- \rightarrow t\bar{t})} \frac{d\sigma(e^+e^- \rightarrow b\dots)}{d \cos \theta_b}, \quad (24)$$

which satisfy the normalization

$$\int_{E_-}^{E_+} W(E_b) dE_b = \int_0^\pi W(\theta_b) \sin \theta_b d\theta_b = 1. \quad (25)$$

These distributions are shown in Fig. 5. It is seen that for the energy distributions in Fig. 5 (left), all the curves cross at the energy  $\tilde{E}_b = \gamma p_b^0$ . This behavior follows from Eq. (13), in particular, the couplings  $\kappa$  and  $\kappa_z$  contribute only to the polarization-dependent part proportional to  $E_b - \tilde{E}_b$  which vanishes at  $E_b = \tilde{E}_b$ . The value of the distribution at the crossing point is  $W(\tilde{E}_b) = (E_+ - E_-)^{-1} = (2V\tilde{E}_b)^{-1}$ , which is  $0.0162 \text{ GeV}^{-1}$  at the  $e^+e^-$  energy 380 GeV.

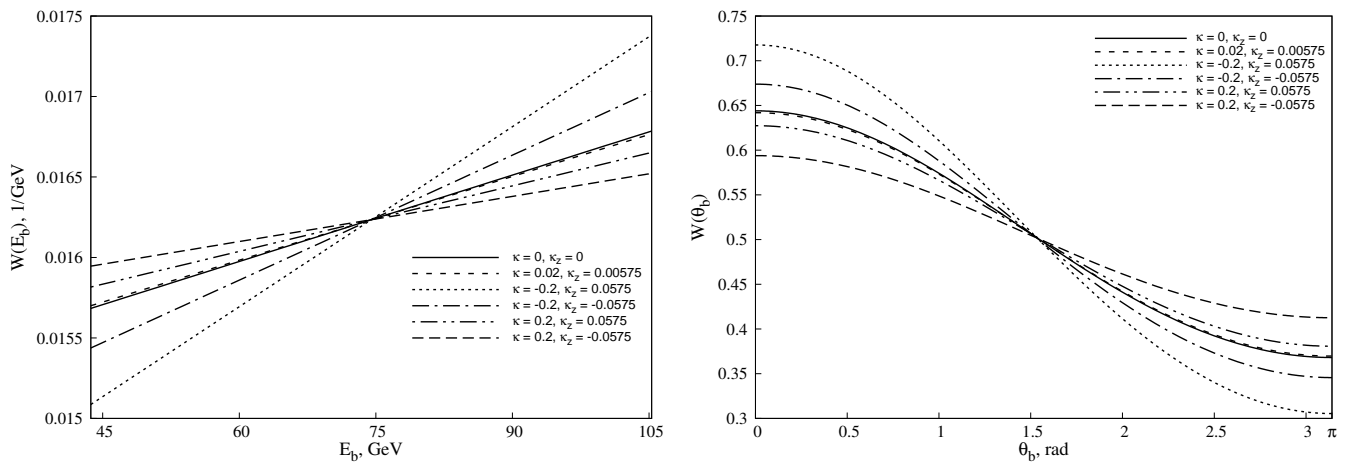


Figure 5: Energy (left panel) and angular (right panel) normalized distributions of the bottom quark at various values of the couplings  $\kappa$ ,  $\kappa_z$ . The  $e^+e^-$  energy is 380 GeV. Only polarization-dependent case is shown.

The angular distribution in Fig. 5 (right) has somewhat different features which follow from Eq. (20). The couplings  $\kappa$  and  $\kappa_z$  enter both polarization-independent and polarization-dependent parts of the distribution. All the curves cross at the angle  $\tilde{\theta}_b \approx \pi/2$ , and the value at the crossing point is  $W(\tilde{\theta}_b) = 1/2$  independently of the  $e^+e^-$  energy. It is also seen that the angular distribution is more sensitive to values of  $\kappa$  and  $\kappa_z$  than the energy distribution.

These simple properties of the energy and angular normalized distributions make them convenient observables for future experimental studies.

## B. Asymmetries

Other important observables, sensitive to the BSM couplings, are the asymmetries of the cross sections. In particular, for the cross section in Eq. (13) one can define the energy asymmetry

$$\mathcal{A}_E = \left( \int_{\tilde{E}_b^-}^{E_+} - \int_{E_-}^{\tilde{E}_b^+} \right) dE_b \frac{d\sigma(e^+e^- \rightarrow b\dots)}{dE_b} \bigg/ \int_{E_-}^{E_+} dE_b \frac{d\sigma(e^+e^- \rightarrow b\dots)}{dE_b}, \quad (26)$$

where the energy  $\tilde{E}_b = \gamma p_b^0$ . This energy is determined by the  $e^+e^-$  invariant energy  $\sqrt{s}$ .

For the cross section in Eq. (20) the forward-backward (FB) asymmetry can be defined as follows

$$\mathcal{A}_{FB} = \left( \int_{\cos\tilde{\theta}}^{+1} - \int_{-1}^{\cos\tilde{\theta}} \right) d\cos\theta_b \frac{d\sigma(e^+e^- \rightarrow b\dots)}{d\cos\theta_b} \bigg/ \int_{-1}^{+1} d\cos\theta_b \frac{d\sigma(e^+e^- \rightarrow b\dots)}{d\cos\theta_b}, \quad (27)$$

where  $\tilde{\theta} = \pi/2$ . Due to the normalizations (15) and (21) the denominators of asymmetries (26) and (27) are fixed by the total  $e^+e^- \rightarrow t\bar{t}$  cross section. In the SM the latter is 0.524 pb at  $\sqrt{s} = 380$  GeV.

The calculated asymmetries are presented in Table II. The values of the BSM couplings are chosen as in Table I. It is seen that for certain coupling constants the energy asymmetry reaches a few percent, and the angular asymmetry takes quite sizable values of about 15-20% that could be accessible in future experiments.

It is of interest to study dependence of the asymmetries on the  $e^+e^-$  energy. The dependence of  $\mathcal{A}_E$  on  $\sqrt{s}$  is plotted in Fig. 6, and the corresponding dependence of  $\mathcal{A}_{FB}$  – in Fig. 7.

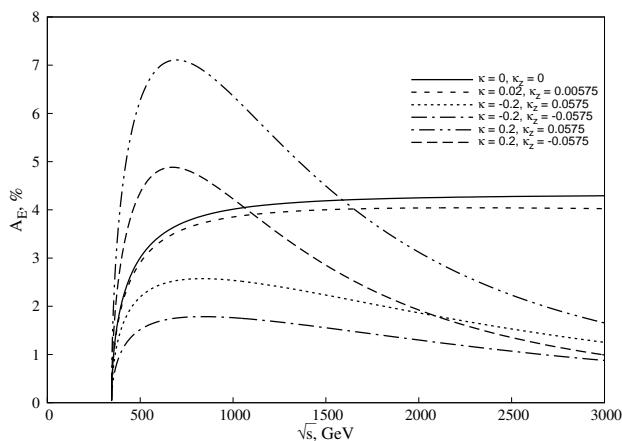
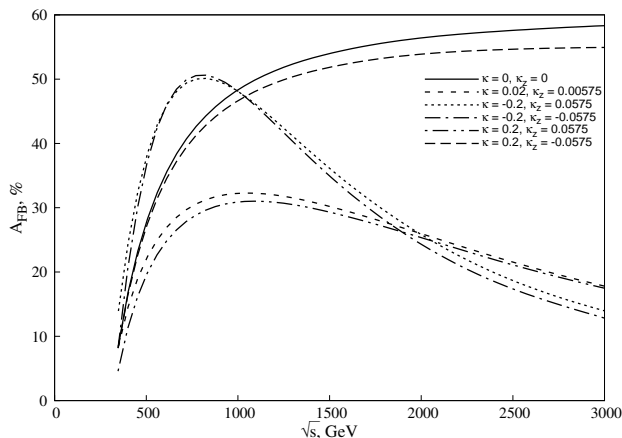
As follows from Fig. 6, the energy asymmetry in the SM is rising up to the energy  $\sim 1$  TeV and then stays almost constant, while the asymmetry beyond the SM has another trend – there is a wide maximum at around energy  $\sqrt{s} \sim 650 - 850$  GeV and then it decreases. This behavior can be of interest for the experimental studies at the CLIC,

Table II: The asymmetries  $\mathcal{A}_E$  and  $\mathcal{A}_{FB}$  in % for various values of the couplings  $\kappa$  and  $\kappa_z$ . The  $e^+e^-$  energy is 380 GeV.

$\kappa$	$\kappa_z$	$\mathcal{A}_E$	$\mathcal{A}_{FB}$
0.0	0.0	1.7	14.0
0.02	0.00575	1.6	14.0
0.2	0.0575	1.3	12.0
0.2	-0.0575	0.9	9.0
-0.2	0.0575	4.0	21.0
-0.2	-0.0575	2.0	16.0

during the next stages of its run, in which the energy is planned to be 1.5 TeV (the 2nd construction stage) and 3 TeV (the 3rd construction stage) with the expected integrated luminosities of  $2.5 \text{ ab}^{-1}$  and  $5 \text{ ab}^{-1}$ , respectively.

Similar behavior is observed for the angular asymmetry in Fig. 7, though the values of  $\mathcal{A}_{FB}$  are an order of magnitude larger than the values of  $\mathcal{A}_E$ .

Figure 6: The energy asymmetry as a function of  $\sqrt{s}$  for various values of the couplings.Figure 7: The angular asymmetry as a function of  $\sqrt{s}$  for various values of the couplings.

Finally, we briefly address the issue of equivalence of the two methods of calculation of the cross section mentioned in the beginning of Sec. II. One has to check the equivalence of Eqs. (1) and (2), though formally they look differently. To calculate the cross section using Eq. (2), we evaluate the  $e^+e^- \rightarrow t\bar{t}$  differential cross section with the polarization

density matrix of the top quark

$$u(p_t, m_t) \bar{u}(p_t, m_t) = \frac{1}{2}(\not{p}_t + m_t)(1 + \gamma^5 \not{\eta}) \quad (28)$$

with  $\not{p}_t = \gamma \cdot p_t$ ,  $\not{\eta} = \gamma \cdot n$  and the four-vector  $n^\mu$  given in (3). Note that in the top-quark rest frame  $n_R^\mu = (0, \alpha_b \vec{n}_{b,R})$ .

Explicit calculation of the differential cross sections in Eqs. (13) and (20) shows that indeed the two ways of evaluation of the cross section lead to the identical results. In view of this we do not present results using Eq. (2).

#### IV. CONCLUSIONS

We studied the spectra of the bottom quark from the decay of the top quark,  $t \rightarrow b W^+$ , produced in the electron-positron annihilation. The formalism used in calculation is based on the method of Ref. [17]. The cross sections of the process  $e^+e^- \rightarrow b \dots$ , as functions of the  $b$ -quark energy and angle with respect to the direction of the electron beam, are derived and calculated. In the calculation, the  $e^+e^-$  energy  $\sqrt{s} = 380$  GeV corresponding to the first construction stage of the CLIC, was chosen.

We investigated the influence of the top-quark polarization, which arises in the  $e^+e^- \rightarrow t\bar{t}$  reaction, on the energy and angular spectra of the bottom quark. In general, the difference between the cross sections for the polarized and unpolarized top quark is not too big, the effect is of the order of 10%. The angular spectrum turns out to be more sensitive to the top-quark polarization than the energy spectrum.

It is shown that the cross section of the  $e^+e^- \rightarrow b \dots$  reaction strongly depends on values of the  $\gamma t\bar{t}$  and  $Z t\bar{t}$  anomalous couplings  $\kappa$  and  $\kappa_z$ . These couplings beyond the SM can take quite sizable values, and we studied how the energy and angular spectra of the  $b$  quark depend on  $\kappa$  and  $\kappa_z$ . It follows from these calculations that the BSM effects can be quite important and perspective for studying the top quark properties.

Several observables, sensitive to these couplings, were considered, namely, the energy and angular normalized distributions, and the energy and angular asymmetries. In particular, the angular asymmetry  $\mathcal{A}_{FB}$  at  $\sqrt{s} = 380$  GeV reaches 10-20%, that can possibly be accessible in future experiments. We also investigated dependence of these asymmetries on the invariant  $e^+e^-$  energy up to  $\sqrt{s} = 3$  TeV. An interesting trend is observed – for the couplings beyond the SM these asymmetries have a maximum at the energy  $\sqrt{s} = 650 - 850$  GeV and then the asymmetries decrease, while in the SM the asymmetries slowly rise with  $e^+e^-$  energy and reach  $\sim 4\%$  for the energy asymmetry and  $\sim 60\%$  for the angular asymmetry. This behavior can be of interest for future studies at the CLIC at the next stages of its run, and for other  $e^+e^-$  colliders.

Finally, equivalence of two methods of calculations of the cross sections, suggested in Ref. [17], was verified. Our explicit calculations shows that these two methods give identical results, as expected.

Although the consideration in the paper was performed for the unpolarized electron and positron, the present method can easily be extended to the case of the polarized electron and positron beams. The next step in future can also be the study of the joint distributions of  $b$  and  $\bar{b}$  quarks from decays of the top quark and antiquark.

#### Acknowledgments

This work was partially conducted in the scope of the IDEATE International Associated Laboratory (LIA). The authors acknowledge partial support by the National Academy of Sciences of Ukraine via the program ‘‘Support for

the development of priority areas of scientific research” (6541230).

- 
- [1] Ties Behnke, James E. Brau, Brian Foster, Juan Fuster, Mike Harrison, James McEwan Paterson, Michael Peskin, Marcel Stanitzki, Nicholas Walker, and Hitoshi Yamamoto. The International Linear Collider Technical Design Report - Volume 1: Executive Summary. 6 2013.
- [2] M Aicheler, P Burrows, M Draper, T Garvey, P Lebrun, K Peach, N Phinney, H Schmickler, D Schulte, and N Toge. A Multi-TeV Linear Collider Based on CLIC Technology: CLIC Conceptual Design Report. 10 2012.
- [3] Aleksander Filip Zarnecki. News on the CLIC physics potential. *PoS, ALPS2019*, 2019.
- [4] Aleksander Filip Zarnecki. On the physics potential of ILC and CLIC. In *19th Hellenic School and Workshops on Elementary Particle Physics and Gravity*, 4 2020.
- [5] Lyn Evans and Shinichiro Michizono. The International Linear Collider Machine Staging Report 2017. 11 2017.
- [6] M.J. Boland et al. Updated baseline for a staged Compact Linear Collider. 8 2016.
- [7] I.V. Truten and A.Yu. Korchin. The top-quark polarization beyond the Standard Model in electron-positron annihilation. *Int. J. Mod. Phys. A*, 34(12):1950067, 2019.
- [8] T. Arens and L.M. Sehgal. Energy correlation and asymmetry of secondary leptons in  $e^+e^- \rightarrow t\bar{t}$ . *Phys. Rev. D*, 50:4372–4381, 1994.
- [9] T. Arens and L.M. Sehgal. Secondary leptons as probes of top quark polarization in  $e^+e^- \rightarrow t\bar{t}$ . *Nucl. Phys. B*, 393:46–64, 1993.
- [10] Bohdan Grzadkowski and Zenro Hioki. Energy spectrum of secondary leptons in  $e^+e^- \rightarrow t\bar{t}$ : Nonstandard effects and CP violation. *Nucl. Phys. B*, 484:17–32, 1997.
- [11] Bohdan Grzadkowski and Zenro Hioki. Angular distribution of leptons in general  $t\bar{t}$  production and decay. *Phys. Lett. B*, 529:82–86, 2002.
- [12] E. Christova. CP violating asymmetries of  $b$  quarks and leptons in  $e^+e^- \rightarrow t\bar{t}$  and supersymmetry. *Int. J. Mod. Phys. A*, 14:1–24, 1999.
- [13] Alfred Bartl, Ekaterina Christova, and Walter Majerotto. CP violating asymmetries in top quark production and decay in  $e^+e^-$  annihilation within the MSSM. *Nucl. Phys. B*, 460:235–251, 1996. [Erratum: *Nucl.Phys.B* 465, 365–365 (1996)].
- [14] A. Bartl, E. Christova, T. Gajdosik, and W. Majerotto. CP violating angular asymmetries of  $b$  and  $\bar{b}$  quarks in  $e^+e^- \rightarrow t\bar{t}$ . *Phys. Rev. D*, 58:074007, 1998.
- [15] A. Bartl, E. Christova, T. Gajdosik, and W. Majerotto. CP violating energy asymmetries of  $b$  and  $\bar{b}$  quarks in  $e^+e^- \rightarrow t\bar{t}$ . *Phys. Rev. D*, 59:077503, 1999.
- [16] J.A. Aguilar-Saavedra. A Minimal set of top anomalous couplings. *Nucl. Phys. B*, 812:181–204, 2009.
- [17] S. Kawasaki, T. Shirafuji, and S.Y. Tsai. Productions and decays of short-lived particles in  $e^+e^-$  colliding beam experiments. *Prog. Theor. Phys.*, 49:1656–1678, 1973.
- [18] Ekaterina Christova and Dimitar Draganov. The top quark polarization in the angular and energy distributions of the  $b$  quarks in  $e^+e^- \rightarrow t\bar{t}$ . *Phys. Lett. B*, 434:373–378, 1998.
- [19] V.B. Berestetskii, E.M. Lifshitz, and L.P. Pitaevskii. *QUANTUM ELECTRODYNAMICS*, volume 4 of *Course of Theoretical Physics*. Pergamon Press, Oxford, 1982.
- [20] J.G. Korner, A. Pilaftsis, and M.M. Tung. One Loop QCD Mass effects in the production of polarized bottom and top quarks. *Z. Phys. C*, 63:575–579, 1994.
- [21] S. Groote, J.G. Korner, and M.M. Tung. Longitudinal contribution to the alignment polarization of quarks produced in  $e^+e^-$  annihilation: An  $O(\alpha_s)$  effect. *Z. Phys. C*, 70:281–290, 1996.
- [22] S. Groote and J.G. Korner. Transverse polarization of top quarks produced in  $e^+e^-$  annihilation at  $O(\alpha_s)$ . *Z. Phys. C*, 72:255–261, 1996. [Erratum: *Z.Phys.C* 70, 531E (2010)].
- [23] John B. Stav and Haakon A. Olsen. Massive quark - anti-quark production with gluon radiative effects in high-energy spin polarized electron - positron collisions. *Phys. Rev. D*, 54:817–827, 1996.
- [24] Haakon A. Olsen and John B. Stav. Quark and anti-quark polarization effects in  $q\bar{q}$  and  $q\bar{q}g$  final states in high-energy collisions of polarized electrons and positrons. *Phys. Rev. D*, 56:407–425, 1997.

- [25] W. Bernreuther, R. Bonciani, T. Gehrmann, R. Heinesch, T. Leineweber, P. Mastrolia, and E. Remiddi. QCD corrections to static heavy quark form-factors. *Phys. Rev. Lett.*, 95:261802, 2005.